ACI JOURNAL TECHNICAL PAPER

Title no. 80-13

Uncertainty Analysis of Creep and Shrinkage Effects in Concrete Structures

by Henrik O. Madsen and Zdeněk P. Bažant

A simple probabilistic model, which allows calculation of simple statistics for shrinkage and creep effects for structural elements, is presented. The statistics can be, in particular, the mean value function and the covariance function (including the variance function), which seem to be the most interesting statistics for serviceability analysis. Any deterministic creep and shrinkage formula can be the basis for probabilistic creep and shrinkage models. The formulas are randomized by introducing the entering parameters as random variables and by further introducing random model uncertainty factors to characterize the incompleteness or inadequacy of the deterministic formulas. Statistics for the model's uncertainty factors are derived by a comparison between available test data and predictions for these tests by the formulas. The creep and shrinkage formulas developed by Bažant and Panula (BP model) are chosen.

Structural analysis can be carried out by any conventional deterministic method. In this paper, the analysis is performed by a matrix method which gives essentially exact results if the time discretization is close enough. A large number of examples of practical relevance demonstrates the potential of the method. Some of the examples show that structural effects which in a deterministic anaylsis almost vanish can have a very large uncertainty, which should be taken into account in practical design.

Keywords: concrete construction; **creep properties;** mathematical models; probability theory; reliability; **shrinkage; structural analysis; structural members;** viscoelasticity.

The analysis of uncertainties in the prediction of shrinkage and creep effects in concrete structures has gained wide interest in recent years. This is quite natural since concrete strength and elasticity are already being treated as random properties while actually the scatter in these properties is not as large as the scatter in shrinkage and creep properties. Although many sources contribute, there are basically two types of uncertainty related to the shrinkage and creep processes. These are referred to as the external uncertainty and the internal uncertainty.[1] The external or parameter uncertainty arises from the uncertainty in the influencing parameters such as those representing environment and concrete composition. The internal uncertainty is that inherent in the microscopic creep processes or creep mechanisms. The external uncertainty is generally believed to be the main type. Models for the description of internal uncertainty are proposed in References 1 and 3. However, only a few test results exist for validation of these models and for parameter estimation.

If no internal uncertainty was present, deterministic relations between the environmental and concrete composition parameters, and shrinkage and creep should in principle exist. Due to the complexity of the phenomena these relations have not quite been determined so far. Many approximate relations have been proposed on the basis of physical considerations and test results. No matter which relation is chosen, a model uncertainty is, however, introduced and must be taken into account.

The proposed creep and shrinkage formulas are based on test results obtained with fairly small test specimens, usually loaded uniaxially in pure compression. In structural analysis concrete is usually considered homogenous although there exist within the cross sections large variations in pore relative humidity, temperature, and degree of hydration, giving rise to self-equilibrated stresses, microcracking, and cracking. The creep and shrinkage formulas can therefore give only some averaged properties of the cross section and an additional uncertainty is thus introduced.

Other important sources of uncertainty come from structural analysis. For practical reasons a linear creep law is normally adopted so that the principle of superposition can be used. This may often be a good approximation for service stresses less than 40 to 50 percent of the ultimate compressive strength, but this still adds to the uncertainty of the predictions.

Even assuming homogeneity of concrete, linearity of the creep law, and validity of the ordinary bending theory, calculation of structural effects may still be too complicated. In addition to the highly accurate numerical methods based on time step integration, various simplified methods are therefore used; these especially in-

Received Mar. 17, 1982, and reviewed under Institute publication policies.
Copyright © 1983, American Concrete Institute. All rights reserved, including the making of copies unless permission is obtained from the copyright proprietors. Pertinent discussion will be published in the January-February 1984 ACI JOURNAL if received by Oct. 1, 1983.

Henrik O. Madsen is a senior research engineer, Section for Reliability of Structures, Det norske Veritas. He earned his doctorate from the Technical University of Denmark in 1979 and then joined the civil engineering faculty, Engineering Academy of Denmark, as an associate professor in applied mathematics until 1982. In 1982, Dr. Madsen was awarded the Ostenfeld gold medal for his work on fatigue reliability. He is a coauthor of the book Methods in Structural Reliability, *published in 1983.*

Zdeněk P. Bažant, FACI, is a professor and director, Center for Concrete and Geomaterials, Northwestern University. Dr. Bažant is a Registered Structural Engineer, serves as consultant to Argonne National Laboratory and several other firms, and is on editorial boards of five journals. His works on concrete and geomaterials, inelastic behavior, fracture, and stability have been recognized by a RILEM medal, ASCE Huber Prize and T. Y. Lin Award, IR-100 Award, Guggenheim Fellowship, Ford Foundation Fellowship, and election as Fellow of American Academy of Mechanics.

clude the effective modulus method and the rate-of-flow method. Additional uncertainty caused by using one of these simplified methods is reported in Reference 4.

This paper investigates the external uncertainty in the shrinkage and creep functions and the model uncertainties related to choosing one specific set of shrinkage and creep formulas. A practical method for calculating simple statistics for shrinkage and creep effects for structural elements is presented. The probabilistic method adopted is very simple and, in principle, only requires averaging of a certain number of results from deterministic calculations.

The main objective is to quantify the effect that the correlation between the parameters in different cross sections of the same concrete structure has on the total uncertainty. This effect is illustrated by a number of relevant examples.

Loads, geometrical parameters, and steel parameters are assumed to be deterministic and known; only the influence of varying concrete and environmental parameters is analyzed.

SHRINKAGE AND CREEP FORMULAS

Many prediction formulas for shrinkage and creep have been suggested both in literature and in national and international codes. A common feature of all the formulas is that none of them predict creep and shrinkage perfectly, although some formulas are definitely more accurate than others. The amount of information on the input parameters such as environmental conditions and concrete composition varies considerably from formula to formula. This is not bad because ideally a hierarchy of formulas should be available, demanding increasing amounts of information on the input parameters and in return giving more reliable predictions.

In this study the formulas developed by Bažant and Panula (BP formulas[5]) are chosen. In comparisons of test results with predictions from different formulas, these formulas showed the best agreement.[6] The BP formulas are to a greater extent based on physical considerations than other formulas. Two main advantages of the BP formulas are that they are equally reliable for a large variety of concrete compositions and environmental conditions and that they predict future developments of creep and shrinkage with good accuracy if one or two short-time measurements have been made.

The BP formulas are given in detail in Reference 5. In short, they are, for shrinkage

$$\epsilon_{sh}(t,t_o) = \epsilon_{sh\infty}\, k_h\, S(t,t_o) \tag{1}$$

and for creep

$$J(t,t') = \frac{1}{E_o} + C_o(t,t') + C_d(t,t',t_o) - C_p(t,t',t_o) \tag{2}$$

Here ϵ_{sh} = shrinkage strain; t_O = age of concrete when drying begins; $J(t,t')$ = compliance function (also called the creep function) = strain at age t caused by a uniaxial unit stress acting since concrete age t'; E_O = asymptotic modulus ($\simeq 1.5\, E_c$ where E_c = conventional elastic modulus of concrete); C_O, C_d, C_p = functions describing basic creep (creep at constant temperature and humidity), increase of creep during drying, and decrease of creep after drying; $C_O(t,t') = (\phi_1/E_O)\,(t'^{-m} + \alpha)\,(t-t')^n$ (double power law) where ϕ_1, m, n, and α = parameters, depending on the type of concrete; C_d = function similar to S; and C_p = function similar to C_O; k_h = function of relative humidity h, defined as $1 - h^3$ if $h \leqslant 0.98$, or else $- 0.2$; and S = empirical function of the variable $(t-t_O)/\tau_{sh}$ where τ_{sh} = shrinkage-square half time, proportional to the square of the dimension of the cross section, $S(t,t_O) = [1 + \tau_{sh}/(t-t_O)]^{-1/2}$ where τ_{sh} = shrinkage-square half time = const. $\times (k_S D)^2$, $D = 2 \times$ volume-to-surface ratio, and k_S = factor taking into account the shape of cross section.

The influences of the type and composition of concrete and of environmental variables (relative humidity h and temperature T) are described by empirical or semiempirical formulas[5] which yield coefficients k_h, $\epsilon_{sh\infty}$, τ_{sh}, E_O, ϕ_1, m, n, and α and functions S, C_O, C_d, and C_p. These formulas involve the basic variables listed in Table 1. A computer program for determining all these variables and functions according to the BP formulas is available.[7]

The mean 28 day cylinder strength is calculated by Bolomey's formula

$$E(f_c') = 27\left(\frac{1}{w/c} - 0.5\right) \text{MPa} \tag{3}$$

Table 1 — Assumed coefficients of variation for influencing parameters

	Parameter	Coefficient of variation
h	mean relative humidity of environment	0.2
h_o	initial relative humidity at which the specimen was in moisture equilibrium before time t_o	~0
T	mean environmental temperature	0.1
D	effective thickness of specimen (2 × area/perimeter of cross section)	~0
k_s	shape factor for specimen	0.05
c	cement content in kg/m³	0.1
w/c	water-cement ratio, by weight	0.1
s/c	sand-cement ratio, by weight	0.1
g/c	gravel-cement ratio, by weight	0.1
a_1	parameter depending on cement type	0
f_c'	28 day cylinder strength	0.1

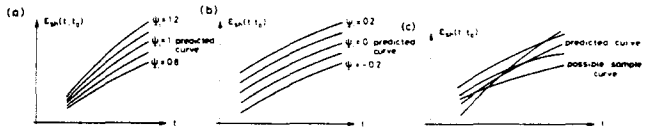

Fig. 1 — Sample curves with different model uncertainty formats

where E denotes expectation and 1MPa = 145.04 psi.

In probabilistic analysis, each variable is represented by its expected value and the coefficient of variation. The numerical values for the coefficients of variation listed in Table 1 were not selected on the basis of precise data, which do not seem to exist, but on an intuitive judgement.

The BP formulas do not predict shrinkage and creep perfectly, and so the resulting model uncertainty will now be analyzed.

MODEL UNCERTAINTY FACTORS

Model uncertainty is accounted for by applying a random factor to each term: shrinkage, basic creep, and drying creep. The formula for shrinkage is then

$$\epsilon_{sh}(t,t_o) = \Psi_1 \epsilon_{sh\infty} k_h S(t,t_o) \quad (4)$$

where Ψ_1 is the model uncertainty factor. Other formats for dealing with model uncertainty could have been chosen, such as applying an additive random variable independent of time

$$\epsilon_{sh}(t,t_o) = \Psi_1 + \epsilon_{sh\infty} k_h S(t,t_o) \quad (5)$$

or applying a multiplicative or additive random function of time

$$\epsilon_{sh}(t,t_o) = \Psi_1(t) \epsilon_{sh\infty} k_h S(t,t_o) \quad (6)$$

$$\epsilon_{sh}(t,t_o) = \Psi_1(t) + \epsilon_{sh\infty} k_h S(t,t_o) \quad (7)$$

With the formats of Eq. (4) or (5), a measured curve ought to correspond to one value of Ψ_1 independent of time [see Fig. 1(a) and (b)]. With the formats of Eq. (6) and (7), measured and predicted curves can differ much more in their shape [see Fig. 1(c)]. A comparison between predicted and measured curves suggests that Eq. (4) provides a sufficiently good description. The mean value and coefficient of variation of a time averaged value of Ψ_1 are estimated in Reference 6 in which the test data are represented by a hand-smoothed curve and are compared to the predicted curve at discrete times, usually one or two time points per decade in the logarithmic time scale.

The model uncertainty for the creep function is assigned in a similar way and the formula for the creep function is then

$$J(t,t') = \Psi_2\left[\frac{1}{E_o} + C_o(t,t')\right] + \Psi_3[C_d(t,t',t_o) - C_o(t,t',t_o)] \quad (8)$$

The mean values and coefficients of variation of the Ψ-factors [of Eq. (4) and (8)] reported in Reference 6 are

$$\begin{aligned} E[\Psi_1] &= 1; & V_{\Psi_1} &= 0.17 \\ E[\Psi_2] &= 1; & V_{\Psi_2} &= 0.24 \\ E[\Psi_3] &= 1; & V_{\Psi_3} &= 0.16 \end{aligned} \quad (9)$$

Due to the way the statistics for the Ψ-factors are determined, they reflect three sources of uncertainty and each Ψ is consequently written as

$$\Psi_i = \Psi_i^* \Psi_\alpha \Psi_\beta \, (i = 1,2,3) \quad (10)$$

where Ψ_i^* = factor due to inadequacy of the prediction formula; Ψ_α = factor due to internal uncertainty; Ψ_β = factor due to measurement errors and uncertainty in the laboratory (or site) environment. The factors to be used in Eq. (4) and (8) are Ψ_i, and the coefficients of variations in Eq. (9) must therefore be corrected. The factors in Eq. (10) are assumed independent, and the relation between the coefficients of variation is[10]

$$(1 + V_{\Psi_i}^2) = (1 + V_{\Psi_i^*}^2)(1 + V_{\Psi_\alpha}^2)(1 + V_{\Psi_\beta}^2) \quad (i = 1, 2, 3) \quad (11)$$

Since the test results were hand-smoothed and the laboratory test conditions were well controlled, the coefficient of variation V_{Ψ_β} is estimated as 0.05. Scant data are available for the estimation of V_{Ψ_α}, but the results in References 11, 12, and 13 indicate that a value between 0.06 and 0.10 is reasonable for test specimens. In the examples reported later in this paper, the following corrected values obtained from the foregoing information and from Eq. (9) are therefore used

Shrinkage	$E[\Psi_1] = 1;$	$V_{\Psi_1} = 0.14$	(corrected values)
Basic creep	$E[\Psi_2] = 1;$	$V_{\Psi_2} = 0.23$	
Drying creep	$E[\Psi_3] = 1;$	$V_{\Psi_3} = 0.13$	

(12)

The coefficients of variation V_Ψ reported in Reference 6 are based on numerous test series involving a large variety of external parameters. Leaving out some test series would reduce the coefficients of variation drastically, but to do that would be a dubious matter. Instead, a weighting procedure for the individual test series, in which the weights would be assigned according to the similarity with the particular concrete and environmental parameters at hand, should be developed. It appears that this could be done within a Bayesian framework. (This approach, presently pursued by J. C. Chern at Northwestern University, is, however, beyond the scope of this paper.)

CALCULATION OF STRUCTURAL EFFECTS

Creep law is assumed linear. The principle of superposition is then valid and the uniaxial relation between stress σ and strain ϵ is[8]

$$\epsilon(t) - \epsilon^o(t) = \int_o^t J(t,t') \, d\sigma(t') \quad (13)$$

in which t = time representing the age measured from the set of concrete; $J(t,t')$ = compliance function (also called creep function) = strain at time t caused by a unit constant stress acting since time t'; and ϵ^o = stress-independent strain due to shrinkage and thermal effects.

With this creep law the solution of structural analysis problems leads to Volterra integral equations. In Reference 4 various methods giving exact and approximate results are compared. To obtain accurate results, numerical step-by-step methods are most efficient. In these methods the time interval $(t_o, \ldots, t_n)$ of interest is divided by discrete times $t_1, t_2, \ldots, t_n$ into time steps $\Delta t_i = t_i - t_{i-1}$. The integral relation in Eq. (13) may then be approximated by

$$\epsilon_i - \epsilon_i^o = \sum_{j=1}^{i} \frac{1}{2} [J(t_i,t_j) + J(t_i,t_{j-1})] \Delta\sigma_j \qquad (14)$$

where subscripts i, j refer to times t_i, t_j or to time steps ending at these times, e.g., $\epsilon_i = \epsilon(t_i)$, and $\Delta\sigma_j = \sigma(t_j) - \sigma(t_{j-1})$. The principles for choosing the division points are given in References 8 and 15. Eq. (14) is applicable even when some stress increments are instantaneous, in which case the corresponding time step is of zero duration. Accuracy of the method is generally very good even for a small number of time intervals. For a moderate number of time points, the results can be considered as exact solutions of the integral equations.[8,15,16]

Structural analysis with the stress-strain relation in Eq. (14) may be reduced to a succession of incremental elastic analyses for the individual time steps.[4,8,15,16] The solution from Reference 4 will be applied here in a matrix form,[17] convenient for the analyst, in which all time steps are solved simultaneously. In contrast to the usual step-by-step solution,[8,4,15,16] such an approach, admittedly, wastes computer time and storage, but this is unimportant for structures with few unknowns, which are of interest here.

Grouping ϵ_i and $\Delta\sigma_i$ in column matrixes $\underline{\epsilon}$ and $\Delta\underline{\sigma}$,* we may rewrite Eq. (14) as

$$\underline{\epsilon} - \underline{\epsilon}^o = \boldsymbol{J}\,\Delta\underline{\sigma} \qquad (15)$$

in which

$$\boldsymbol{J} = \left[\frac{1}{2} [J(t_i,t_j) + J(t_i,t_{j-1})]\right] = (i \times i) \text{ square matrix}$$

Similarly, $\sigma_i = \Sigma\Delta\sigma_j$ can be written as

$$\underline{\sigma} = \boldsymbol{L}\,\Delta\underline{\sigma} \qquad (16)$$

in which $\underline{\sigma} = \{\sigma_i\}$ and $\boldsymbol{L} = (\mathbf{1}_{i \leqslant j})$ = a square matrix whose elements are 1 if $i \leqslant j$, and otherwise are 0. Eq. (15) may then be written as

$$\underline{\epsilon} - \underline{\epsilon}^o = \boldsymbol{E}_c^{-1}\,\underline{\sigma}_c \qquad (17)$$

where

$$\boldsymbol{E}_c^{-1} = \boldsymbol{J}\boldsymbol{L}^{-1} \qquad (17a)$$

The formal similarity of Eq. (17) with Hooke's law reflects the analogy between linearly elastic and linearly viscoelastic materials.[8] As demonstrated in Reference 17, the matrix formulation allows a convenient algebraic treatment of linearly viscoelastic structures (with not too many unknowns), similar to that for linearly elastic problems.

A simple application of the matrix notation may now be shown. Shrinkage of a plain concrete bar is completely restrained causing tensile concrete stresses which are modified by creep. The governing equation is

$$\epsilon(t) = \epsilon_{sh}(t) + \int_o^t J(t,t')d\sigma(t') = 0 \qquad (18)$$

which in matrix formulation reads

$$\underline{\epsilon} = \underline{\epsilon}_{sh} + \boldsymbol{E}_c^{-1}\,\underline{\sigma} = 0 \qquad (19)$$

and from which the concrete stress is found to be

$$\underline{\sigma} = -\boldsymbol{E}_c\,\underline{\epsilon}_{sh} \qquad (20)$$

Due to uncertainties in shrinkage and creep properties, the matrix $\boldsymbol{E}_c$ and the vector $\underline{\epsilon}_{sh}$ are both uncertain.

It may be noted that Eq. (17), on which all the present structural analysis is based, is also applicable for approximate solution by the age-adjusted effective modulus method. In that case, $\boldsymbol{E}_c^{-1}$ becomes a diagonal matrix with diagonal elements $1/E_c''(t_i,t_o)$, in which $E_c''(t_i,t_o)$ is the age-adjusted effective modulus.[8] Advantages of this method are that it allows approximate solution of the structural response at a certain time t_i without solving the response for the preceding times, and that the matrix inversion and multiplication indicated in Eq. (17a) need not be carried out. These advantages make hand calculations feasible; they are, however, insignificant when a computer is used.

UNCERTAINTY ANALYSIS

Before deciding on the type of uncertainty analysis, a number of observations can be made. Creep and shrinkage effects are mainly considered in serviceability analysis, and interest is therefore in the variations close to the mean values rather than extreme values. The relation between creep effects and basic variables is highly nonlinear. The number of basic variables is very large, and for the set of basic variables, hardly more than second moment information is available, i.e., means, variances, and covariances. It then appears that a satisfactory characterization of creep effects consists in achieving good estimates of the mean value at any time, the covariances between values at any two times, and for each basic variable a measure of the relative importance for the creep effect of variations of this parameter.

Previous work[10] gives second moment analysis tools which are directly applicable in connection with the matrix method outlined here for the calculation of structural effects. Application of these tools is demonstrated

*Editor's note — A single line under a Greek letter indicates a matrix quantity.

in Reference 18; they are even applicable when some basic variables are uncertain processes rather than uncertain variables. Although the method is conceptually very simple, serious computational difficulties arise, however, when several correlated uncertain matrixes and their inverse matrixes are dealt with simultaneously, as is the case of this paper's examples. Other, simpler uncertainty analysis methods will therefore be considered.

In the creep and shrinkage models chosen, all basic variables $\underline{\theta} = (\theta_1, \ldots, \theta_k)$ are random variables. Given the value of $\underline{\theta}$, any creep effect is then represented as a function of time. Let the creep effect be denoted $X(\underline{\theta},t)$. A linearization of $X(\underline{\theta},t)$ around the mean value point $E[\underline{\theta}]$ gives the following mean value and covariance function[10]

$$E[X(\underline{\theta},t)] \doteq X(E[\underline{\theta}],t) \tag{21}$$

$$\mathrm{Cov}[X(\underline{\theta},t_1),X(\underline{\theta},t_2)] \doteq$$
$$\doteq \sum_{i=1}^{k}\sum_{j=1}^{k} \frac{\partial X}{\partial \theta_i}(E[\underline{\theta}],t_1)\,\frac{\partial X}{\partial \theta_j}(E[\underline{\theta}],t_2)\,\mathrm{Cov}[\theta_i,\theta_j] \tag{22}$$

where Cov denotes the covariance and the sign $\doteq$ symbolizes the linearization of the right-hand side. Due to the complex functional relationship between the creep effects and the basic variables, the partial derivatives in Eq. (22) are, however, difficult to calculate analytically. If the partial derivatives are calculated numerically, the method becomes less attractive than the method which is proposed next and is based on point estimates for probability moments.

Let θ be a random variable with mean value μ and standard deviation s, and let the interest be focused on the mean value of some function $g(\theta)$. Possible observations $\theta_{(1)}, \theta_{(2)}, \ldots, \theta_{(m)}$ of θ are chosen together with m nonnegative numbers $p_1, p_2, \ldots, p_m$, the sum of which equals 1. The mean value of $g(\theta)$ may then be assigned as

$$E[g(\theta)] = p_1 g(\theta_{(1)}) + p_2 g(\theta_{(2)}) + \ldots + p_m g(\theta_{(m)}) \tag{23}$$

Since the mean value and variance of θ are given, the $\theta_{(m)}$ and p_n cannot be chosen arbitrarily but must satisfy the conditions

$$\left.\begin{aligned} E[\theta] &= p_1\theta_{(1)} + p_2\theta_{(2)} + \ldots + p_m\theta_{(m)} = \mu \\ E[\theta^2] &= p_1\theta^2_{(1)} + p_2\theta^2_{(2)} \\ &\quad + \ldots + p_m\theta^2_{(m)} = \mu^2 + s^2 \end{aligned}\right\} \tag{24}$$

The simplest choice consists in choosing two points $\theta_{(1)}, \theta_{(2)} = \mu \pm s$ with both p_n equal to ½ (Fig. 2). Thus, for two-point estimates, the expected value of $g(\theta)$ is assigned as

$$E[g(\theta)] = \tfrac{1}{2}[g(\mu + s) + g(\mu - s)] \tag{26}$$

Use of this procedure as an aid to assign mean values to functions of random variables with some mean values already given was suggested in Reference 14. Reference 10 describes a more formal mathematical setup of a so-called n-mass uncertainty algebra which also includes this procedure. The generalization to two and three dimensions is also shown in Fig. 2. Extensions to four or more dimensions are rather straightforward, but there are here infinitely many possible sets of p-values and it must be checked that no negative p-values are selected.

It is useful to note the validity of the following relations from linear regression analysis

$$E[\theta_i|\theta_j = \mu_j \pm s_j] = \mu_i \pm \rho_{ij}\, s_i \,(i, j = 1, 2, \ldots k) \tag{27}$$

$$\mathrm{Var}[\theta_i|\theta_j = \mu_j \pm s_j] = s_i^2\,(1 - \rho_{ij}^2) \tag{28}$$

where Var denotes the variance, s_i are the standard deviations of random variables θ_i, and ρ_{ij} are their correlation coefficients. An intuitive measure of the relative importance of uncertainty of each parameter is α_i, defined as

$$\alpha_i = \frac{\mathrm{Var}[g(\underline{\theta})] - E[\mathrm{Var}[g(\underline{\theta})|\theta_i]]}{\mathrm{Var}[g(\underline{\theta})]} = \frac{\mathrm{Var}[E[g(\underline{\theta})|\theta_i]]}{\mathrm{Var}[g(\underline{\theta})]}$$
$$= \{\mathrm{Var}[g(\underline{\theta})] - \tfrac{1}{2}\,(\mathrm{Var}[g(\underline{\theta})|\theta_i = \mu_i + s_i]$$
$$+ \mathrm{Var}[g(\underline{\theta})|\theta_i = \mu_i - s_i])\}/\mathrm{Var}[g(\underline{\theta})] \tag{29}$$

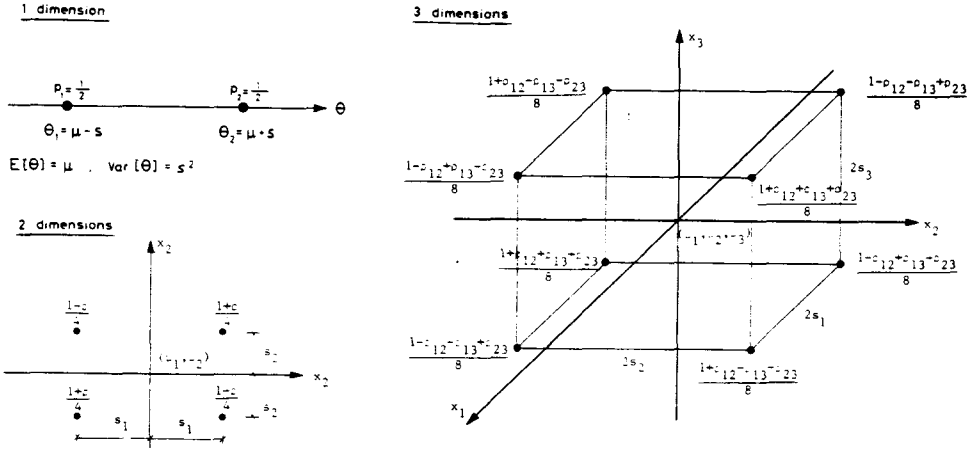

Fig. 2 — Weights and points

Table 2 — Deterministic parameters and mean values of basic variables

t_o	h	h_o	T	D	k_s	a_1	C	w/c	s/c	g/c
10	0.65	1.0	20	100	1.15	1	275	0.56	3.08	4.00

where the last equality is valid for the choice of θs and ps as shown in the figures.

Applying the procedure involves a calculation of creep effects for each of the 2^k possibilities of θ (k being the number of variables). The mean value and the covariance functions are then calculated by the appropriate weighting of results. For a large k, the number of calculations is thus very large, but, as will be seen, the relative importance factor α_i for several basic variables is so small that these variables can just be taken at their mean values.

A third procedure, which can always be used, is simulation. A formal choice of the distribution type of the set of basic variables $\underline{\theta}$ must then be made. Sample θs are then simulated and the corresponding creep effects calculated. The mean value and covariance functions are obtained by giving each sample the same weight. The number of simulations necessary to give good estimates of the mean and covariance functions is not extremely high, but it is difficult to estimate any relative measure of importance for each variable.

The point estimate method seems to be the best one for this application with regard to the information on the input, computation time, and output.

RELATIVE IMPORTANCE FACTORS

Including the three model uncertainty factors, there are 11 basic variables in the shrinkage and creep formulas, Eq. (4) and (8). The relative importance factor defined in Eq. (29) is for the shrinkage function determined for each basic variable. For the creep function this is done only in two cases. The mean values of the basic variable and the deterministic parameters are listed in Table 2. These values are chosen somewhat arbitrarily, but very similar relative importance factors were observed for other choices of parameter values. Coefficients of variation of the basic variables are taken from Table 1 and Eq. (12).

Tables 3 to 5 show that the relative importance factors for the temperature T and the shape factor k_s are very small. These two parameters influence the time scale of shrinkage and creep development rather than the magnitude. The sand-cement ratio s/c and the model uncertainty factor for drying creep Ψ_3 also have very small relative importance factors. In some of the following examples, these four parameters are taken as deterministic, thus reducing the number of random variables and the computer time.

EXAMPLES

We now combine the structural analysis method described in Eq. (13) through (20) with the present uncertainty analysis, considering a number of examples of practical importance. The examples include both non-composite and composite structures. For a noncomposite structure the age of concrete is assumed to be uniform, and so the same creep and shrinkage function is valid for all parts of the structure. A composite structure may comprise reinforcement, and the age and composition of concrete may vary from one part of the structure to another. In each example the structural analysis is briefly described and the values of the variables listed. Results of the calculations are given as the mean value function and the standard deviation function of the structural effects.

Table 3 — Relative importance factors (in percent) for creep formula*

t	10.00	11.00	14.64	31.54	110.0	473.9	2163	10,000
h	0	3	4	6	8	10	11	10
T	0	0	0	0	0	0	0	0
k_s	0	0	0	0	0	0	0	0
C	9	9	9	9	8	8	8	9
w/c	4	9	9	10	10	11	11	10
s/c	1	2	3	3	3	4	4	4
g/c	2	3	3	4	4	4	4	4
Ψ_2	78	67	63	59	53	48	44	44
Ψ_3	0	1	1	1	2	2	3	2
f_c'	2	1	1	1	0	0	0	0
Total	96	95	93	93	88	87	85	83

*t_o = 10 days; t' = 10⁰ days.

Table 4 — Relative importance factors (in percent) for creep formula*

t	100.0	102.0	108.3	134.1	240.7	680.9	2498	10,000
h	0	3	5	7	10	13	15	15
T	0	0	0	0	0	0	0	0
k_s	0	0	0	0	0	0	0	0
C	9	9	9	9	9	8	9	10
w/c	4	7	8	9	10	10	10	9
s/c	1	3	3	3	4	4	4	4
g/c	2	3	3	4	4	4	4	4
Ψ_2	78	68	63	57	50	44	39	38
Ψ_3	0	1	1	2	3	3	4	4
f_c'	2	1	1	1	0	0	0	0
Total	96	95	93	92	90	86	85	84

*t_o = 10 days; t' = 100 days.

Table 5 — Relative importance factors (in percent) for shrinkage formula*

t	11.00	14.64	31.54	110.0	473.9	2163	10,000
h	11	11	11	11	12	13	14
T	1	1	1	1	0	0	0
k_s	1	1	1	1	0	0	0
C	2	2	2	2	1	0	0
w/c	44	44	44	44	44	42	41
s/c	0	0	0	0	0	0	0
g/c	12	12	12	13	14	15	15
Ψ_1	7	7	7	7	8	8	9
f_c'	7	7	7	7	8	9	9
Total	85	85	85	86	87	87	88

*t_o = 10 days.

Restrained shrinkage in a plain concrete bar

The concrete bar of Fig. 3 is considered. Concrete stress due to restrained shrinkage is given in Eq. (20). The parameter values are given in Table 6(a), and results of the calculations are shown in Fig. 3.

Restrained shrinkage in a frame

Fig. 4 shows a plane frame structure which has a uniform cross section and is subjected to shrinkage and creep which causes development of horizontal forces at the supports. Relative displacements of the supports due to shrinkage and the reaction $R(t)$ in the primary stati-

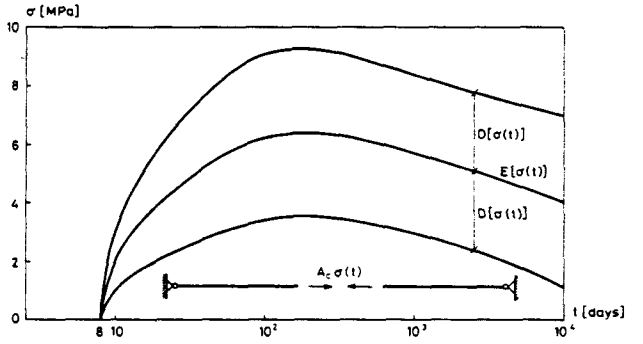

Fig. 3 — Stresses in concrete bar subjected to shrinkage and creep

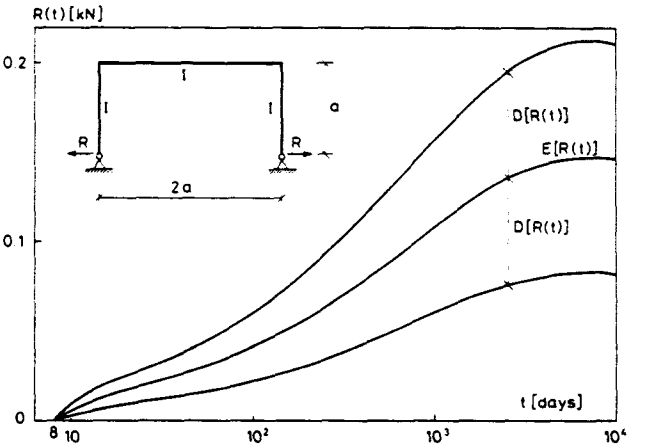

Fig. 4 — Reaction due to restrained shrinkage in frame

cally determinate system are denoted as $\delta_S(t)$ and $\delta_R(t)$, respectively. Since the supports are fixed, the governing compatibility condition is $\delta(t) = \delta_S(t) + \delta_R(t) = 0$. The displacement due to shrinkage is $\delta_S(t) = 2\,a\,\epsilon_{sh}(t)$.

According to the ordinary bending theory, in which shear deformations are neglected, the displacement due to the reaction $R(t)$ is

$$\delta_R(t) = \frac{8a^3}{3I} \int_o^t J(t,t')\,dR(t') \tag{30}$$

In matrix notation, the governing equation is

$$\underline{\delta} = 2a\,\underline{\epsilon}_{sh} + \frac{8a^3}{3I}\,E_c^{-1}\,\boldsymbol{R} = \boldsymbol{0} \tag{31}$$

From this equation, the reaction $\boldsymbol{R}$ is calculated

$$\boldsymbol{R} = -\frac{3I}{4a^2}\,E_c\,\underline{\epsilon}_{sh} \tag{32}$$

Results for a frame with $a = 5$ m (196.9 in.) and $I = 2.13 \cdot 10^{-3}$ m^4 (5117 in.^{4}) are shown in Fig. 4. Parameter values given in Table 6(b) were used in the calculations.

Simply supported beams made continuous

Fig. 5 shows two identical, simply supported concrete beams that are loaded at time $t = t_1$ and coupled (without enforcing any rotations at the beam ends) at $t = t_k$ to form a continuous beam. The change of structural system introduces a redundant bending moment $M(t)$ governed by the compatibility condition $\delta_g(t) + \delta_M(t) = 0$, $t \geq t_k$. This equation expresses the fact that the mutual rotation, due to the load g and the redundant moment $M(t)$, between the two beam ends (in the sense of M) remains unchanged after time t_k. According to the ordinary bending theory, the two rotations are

$$\delta_g(t) = 2\,\frac{gl^3}{24I}[J(t,t_1) - J(t_k,t_1)] \tag{33}$$

$$\delta_M(t) = 2\,\frac{l}{3I} \int_{t_k}^t J(t,t')\,dM(t') \tag{34}$$

In matrix formulation the governing equation is

$$2\,\frac{gl^3}{24I}\,\boldsymbol{c} + 2\,\frac{l}{3I}\,E_c^{-1}\,\boldsymbol{M} = \boldsymbol{0} \tag{35}$$

where the elements in the column matrix $\boldsymbol{c}$ are the values $J(t,t_1) - J(t_k,t_1)$. The solution for $\boldsymbol{M}$ is

$$\boldsymbol{M} = -\frac{l}{8}\,g l^2\,E_c\,\boldsymbol{c} \tag{36}$$

Table 6 — Mean values $E[\ ]$ and coefficients of variation used in examples

Parameter		h	h_o	T	D	k_s	a_1	C	w/c	s/c	g/c	Ψ_1	Ψ_2	Ψ_3	f'_c	t_o
(a)	$E[\ ]$	0.65	1.00	23	50	1.25	1.0	450	0.46	1.66	2.07	1	1	1	—	8
	V	0.2	0	0	0	0	0	0.1	0.1	0	0.1	0.14	0.23	0.13	0.1	—
(b)	$E[\ ]$	0.7	1.00	20	200	1.25	1.0	350	0.4	2.0	3.5	1	1	1	—	8
	V	0.2	0	0	0	0	0	0.1	0.1	0	0.1	0.14	0.23	0.13	0.1	—
(c)	$E[\ ]$	0.65	1.00	20	400	1.10	1.0	350	0.6	2.0	3.0	—	1	1	—	30
	V	0.2	0	0	0	0	0	0.1	0.1	0	0.1	—	0.23	0.13	0.1	—
(d)	$E[\ ]$	0.65	1.00	20	350	1.00	1.0	385	0.42	2.1	2.7	—	1	1	—	7
	V	0.2	0	0	0	0	0	0.1	0.1	0	0.1	—	0.23	0.13	0.1	—
(e)	$E[\ ]$	0.65	1.00	20	345	1.20	1.0	375	0.4	2.0	3.0	1	1	1	—	15
	V	0.2	0	0	0	0	0	0.1	0.1	0	0.1	0.14	0.23	0.13	0.1	—
(f)	$E[\ ]$	0.65	1.00	20	95.6	1.00	1.0	350	0.4	2.0	3.5	1	1	1	—	15
	V	0.2	0	0	0	0	0	0.1	0.1	0.1	0.1	0.14	0.23	0.13	0.1	—
(g)	$E[\ ]$	0.65	1.00	20	250	1.20	1.0	350	0.5	2.0	3.4	—	1	1	—	28
	V	0.2	0	0	0	0	0	0.1	0.1	0	0.1	—	0.23	0.13	0.1	—
(h)	$E[\ ]$	0.65	1.00	20	285	1.00	1.0	385	0.42	2.1	2.7	—	1	1	—	28
	V	0	0	0	0	0	0	0	0	0	0	—	0.23	0	0	—

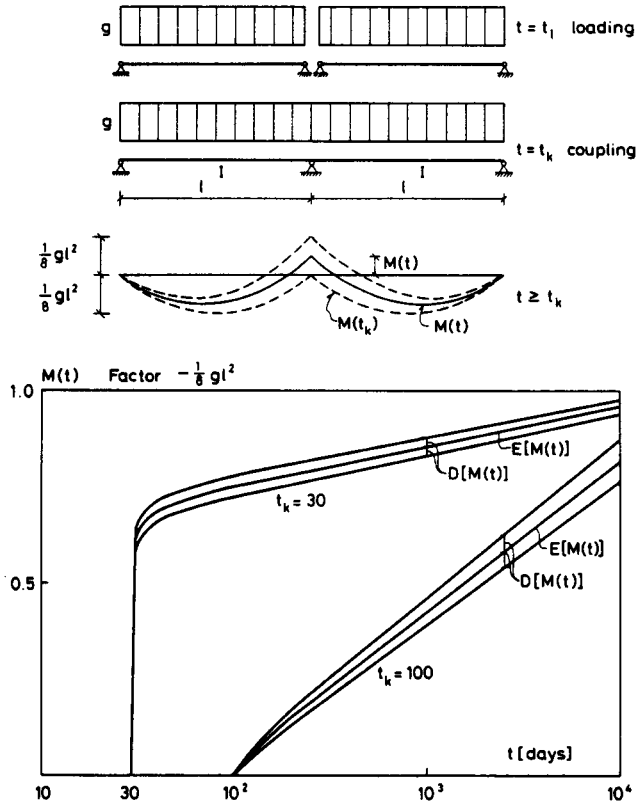

Fig. 5 — Redundant bending moment from coupling of beams

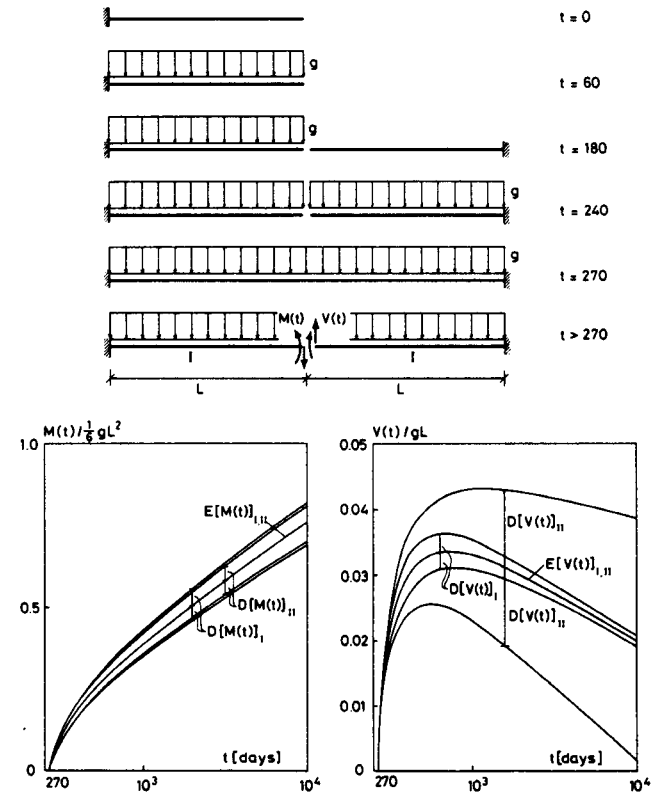

Fig. 6 — Redundant sectional forces from coupling of cantilever beams

Fig. 5 shows the results for two different times t_k of coupling. The parameter values used in the calculations are given in Table 6(c).

Coupling of cantilever beams of different ages

Fig. 6 shows two opposite cantilever beams of different ages, which are connected together at midspan. This causes development of shear forces and bending moments in the connection. The load history is simplified as shown in Fig. 6. The moment $M(t)$ and shear force $V(t)$ may be determined from equations expressing the fact that the mutual displacement and rotation are zero at the connection after the time of coupling. These equations are

$$\frac{1}{8}\frac{gL^4}{I}[J_1(t,60) - J_1(270,60)] + \frac{1}{3}\frac{L^3}{I}\int_{270}^{t} J_1(t,t')\,dV(t') - \frac{1}{2}\frac{L^2}{I}\int_{270}^{t} J_1(t,t')\,dM(t') - \frac{1}{8}\frac{gL^4}{I}[J_2(t-180,60) - J_2(90,60)] + \frac{1}{3}\frac{L^3}{I}\int_{270}^{t} J_2(t-180,t'-180)\,dV(t') + \frac{1}{2}\frac{L^2}{I}\int_{270}^{t} J_2(t-180,t'-180)\,dM(t') = 0 \quad (37)$$

$$-\frac{1}{6}\frac{gL^3}{I}[J_1(t,60) - J_1(270,60)] - \frac{1}{2}\frac{L^2}{I}\int_{270}^{t} J_1(t,t')\,dV(t') + \frac{L}{I}\int_{270}^{t} J_1(t,t')\,dM(t') - \frac{1}{6}\frac{gL^3}{I}[J_2(t-180,60) - J_2(90,60)] + \frac{1}{2}\frac{L^2}{I}\int_{270}^{t} J_2[(t-180,t'-180)\,dV(t')] + \frac{L}{I}\int_{270}^{t} J_2(t-180,t'-180)\,dM(t') = 0 \quad (38)$$

In matrix formulation, these equations may be written as

$$\frac{1}{8}\frac{gL^4}{I}(c_1 - c_2) + \frac{1}{3}\frac{L^3}{I}(E_{c1}^{-1} + E_{c2}^{-1})\,V - \frac{1}{2}\frac{L^2}{I}(E_{c1}^{-1} - E_{c2}^{-1})\,M = O \quad (39)$$

$$-\frac{1}{6}\frac{gL^3}{I}(c_1 + c_2) - \frac{1}{2}\frac{L^2}{I}(E_{c1}^{-1} - E_{c2}^{-1})\,V + \frac{L}{I}(E_{c1}^{-1} + E_{c2}^{-1})\,M = 0 \quad (40)$$

where V and M are the unknown column matrixes of $V(t_i)$ and $M(t_i)$. E_{c1} is determined from $J_1(t,t')$ and E_{c2} from $J_2(t-180,t'-180)$ and where the elements in the column matrix c_1 are $J_1(t,60) - J_1(270,60)$ and in the column matrix c_2 are $J_2(t-180,60) - J_2(90,60)$. The solution is

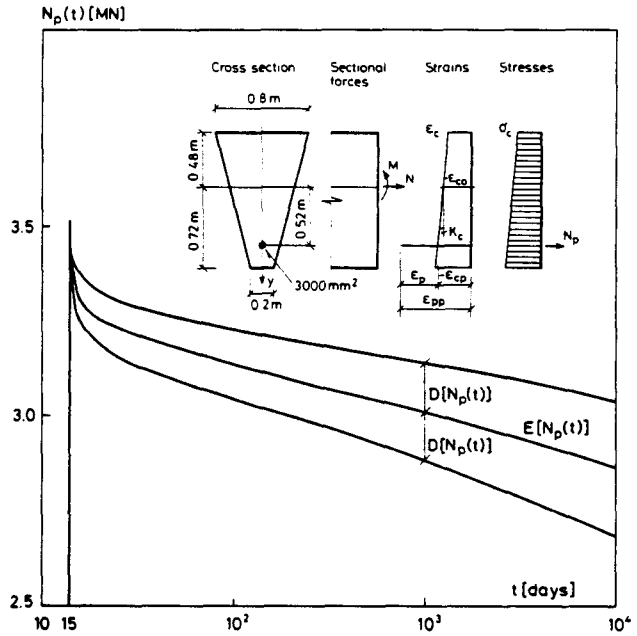

Fig. 7 — Prestress loss in prestressed beam

$$V = gL\ \left[(E_{c1}^{-1} + E_{c2}^{-1})(E_{c1}^{-1} - E_{c2}^{-1})^{-1}(E_{c1}^{-1} + E_{c2}^{-1}) - \frac{3}{4}(E_{c1}^{-1} - E_{c2}^{-1})\right]^{-1}\left[\frac{1}{4}(c_1 + c_2) + \frac{3}{8}(E_{c1}^{-1} + E_{c2}^{-1})(E_{c1}^{-1} - E_{c2}^{-1})^{-1}(c_2 - c_1)\right] \quad (41)$$

$$M = \frac{1}{6}gL^2\ \left[(E_{c1}^{-1} + E_{c2}^{-1}) - \frac{3}{4}(E_{c1}^{-1} - E_{c2}^{-1})(E_{c1}^{-1} + E_{c2}^{-1})^{-1}(E_{c1}^{-1} - E_{c2}^{-1})\right]^{-1}\left\{(c_1 + c_2) + \frac{9}{8}(E_{c1}^{-1} - E_{c2}^{-1})(E_{c1}^{-1} + E_{c2}^{-1})^{-1}(c_2 - c_1)\right\} \quad (42)$$

Parameter values used in the calculations are listed in Table 6(d).

Results are shown in Fig. 6. The curves marked *I* correspond to a situation with identical parameters for both beams. The curves marked II correspond to a situation in which water-cement ratio varies in one cantilever independently of the other, while all other variables are identical for both cantilevers. The effect of varying water-cement ratio on the standard deviation function differs for the two cross-sectional forces.

Bending moment is determined mainly by $(E_{c1}^{-1} + E_{c2}^{-1})$ and $(c_1 + c_2)$ where the terms in each bracket are positively correlated. When the water-cement ratio varies in each cantilever independently, the correlation decreases causing a decrease in the variance. The situation is opposite for the shear force, since it is mainly determined by $(E_{c1}^{-1} - E_{c2}^{-1})$ and $(c_2 - c_1)$. Here a decrease in the correlation between the terms in each bracket causes an increase in the variance.

Prestress loss in a prestressed concrete beam

Fig. 7 shows a symmetric cross section of a prestressed concrete beam subjected to plane compound bending. The prestressing steel consists of one tendon with cross section area $A_p = 3000$ mm² at distance $y_p = 0.52$ from the centroidal axis of the concrete cross section. The prestressing steel is assumed to be linearly elastic, with modulus of elasticity $E_p = 200{,}000$ MN/m² (29×10^6 psi).

In matrix notation, stress-strain relations are

$$\underline{\epsilon}_p = \frac{1}{E_p}\underline{\sigma}_p,\ \underline{\epsilon}_c = E_c^{-1}\underline{\sigma}_c + \underline{\epsilon}_{sh} \quad (43)$$

where the subscripts p and c distinguish between prestressing steel and concrete. The concrete strain distribution is assumed to be planar, and the difference between the steel strain $\underline{\epsilon}_p$ and concrete strain $\underline{\epsilon}_{cp}$ at steel level $y = y_p$ is $\underline{\epsilon}_{pp}$, which defines the prestress. Therefore

$$\underline{\epsilon}_c = \underline{\epsilon}_{co} + \underline{\kappa}_c y,\quad \underline{\epsilon}_p = \underline{\epsilon}_{pp} + \underline{\epsilon}_{cp} \quad (44)$$

Equilibrium conditions relating the normal forces N_p and N_c in steel and concrete, bending moment M_c in concrete to the total normal force N, and bending moment M are

$$N = N_p + N_c,\quad M = N_p Y_p + M_c \quad (45)$$

where the column matrixes $\underline{N}$, $\underline{N}_c$, $\underline{M}_c$, $\underline{N}$, and $\underline{M}$ group the discrete values at times t_i. Since the concrete stresses must be linearly distributed

$$\underline{\sigma}_c = \frac{1}{A_c}\underline{N}_c + \frac{y}{I_c}\underline{M}_c,\quad \sigma_p = \frac{1}{A_p}N_p \quad (46)$$

These equations are solved with respect to the steel force N_p

$$N_p = A_p E_p \left[I + \left(\frac{A_p}{A_c} + \frac{A_p y_p^2}{I_c}\right)E_p E_c^{-1}\right]^{-1} \left\{\underline{\epsilon}_{pp} + \underline{\epsilon}_{sh} + E_c^{-1}\left(\frac{N}{A_c} + \frac{My_p}{I_c}\right)\right\} \quad (47)$$

in which I is the unit matrix. For the cross section of Fig. 7 we have $A_c = 0.60$ m² (930 in.²) and $I_c = 63.36 \cdot 10^{-3}$ m⁴ (152,200 in.⁴). The prestress strain $\underline{\epsilon}_{pp}$ was taken constant in time and equal to $6 \cdot 10^{-3}$ (bonded reinforcement), and the cross-sectional forces were taken constant in time as $N = 0$, $M = 1$ MNm (8851 kip-in.). Shrinkage and creep parameters are listed in Table 6(e). Results for the steel force are shown in Fig. 7.

Stress redistribution in steel-concrete composite beam

Fig. 8 shows a symmetric cross section of a composite steel-concrete beam subjected to compound bending. The governing equations in matrix formulation are, with the notations defined in Fig. 8, as follows.[4]

Stress strain relations

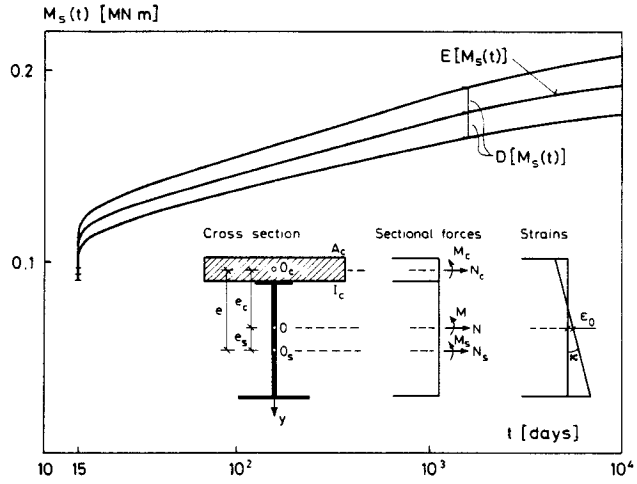

Fig. 8 — Changes of steel girder moments in steel-concrete composite beam

$$\underline{\epsilon}_s(y) = \frac{1}{E_s}\,\underline{\sigma}_s(y), \quad \underline{\epsilon}_c(y) = E_c^{-1}\,\underline{\sigma}_c(y) + \epsilon_{sh} \tag{48}$$

Strain distribution

$$\underline{\epsilon}_s(y) = \underline{\epsilon}_c(y) = \underline{\epsilon}_o + \underline{\kappa}\, y \tag{49}$$

Equilibrium conditions

$$N = N_c + N_s, \quad M = M_s + N_s e_s + M_c - N_c e_c \tag{50}$$

Stress distributions

$$\underline{\sigma}_s(y) = \frac{N_s}{A_s} + \frac{M_s}{I_s}(y - e_s),$$
$$\underline{\sigma}_c(y) = \frac{N_c}{A_c} + \frac{M_c}{I_c}(y + e_c) \tag{51}$$

These equations are solved with respect to the steel force N_s and bending moment M_s

$$N_s = \left[\left(E_c\frac{I_c}{E_sI_se} + I\frac{1}{e}\right)^{-1} + \frac{I_sE_s}{e}\left(I\frac{1}{E_sA_s} + E_c^{-1}\frac{1}{A_c}\right)\right]^{-1} \left\{\left(E_c\frac{1}{E_sI_s} + I\frac{1}{I_c}\right)^{-1}\left(\frac{M + Ne_c}{I_c}\right) + \frac{I_sE_s}{e}\left(E_c^{-1}\frac{N}{A_c} + \epsilon_{sh}\right)\right\}$$

$$M_s = \left[\left(E_c\frac{I_c}{E_sI_se} + I\frac{1}{e}\right) + \frac{e}{I_sE_s}\left(I\frac{1}{E_sA_s} + E_c^{-1}\frac{1}{A_c}\right)^{-1}\right]^{-1} \left\{\frac{M + Ne_c}{e} - \left(I\frac{1}{E_sA_s} + E_c^{-1}\frac{1}{A_c}\right)^{-1}\left(E_c^{-1}\frac{N}{A_c} + \epsilon_{sh}\right)\right\} \tag{50}$$

Cross-sectional forces are taken as constant in time, with $N = 0$ and $M = 0.284$ MNm (8851 kip-in.). The

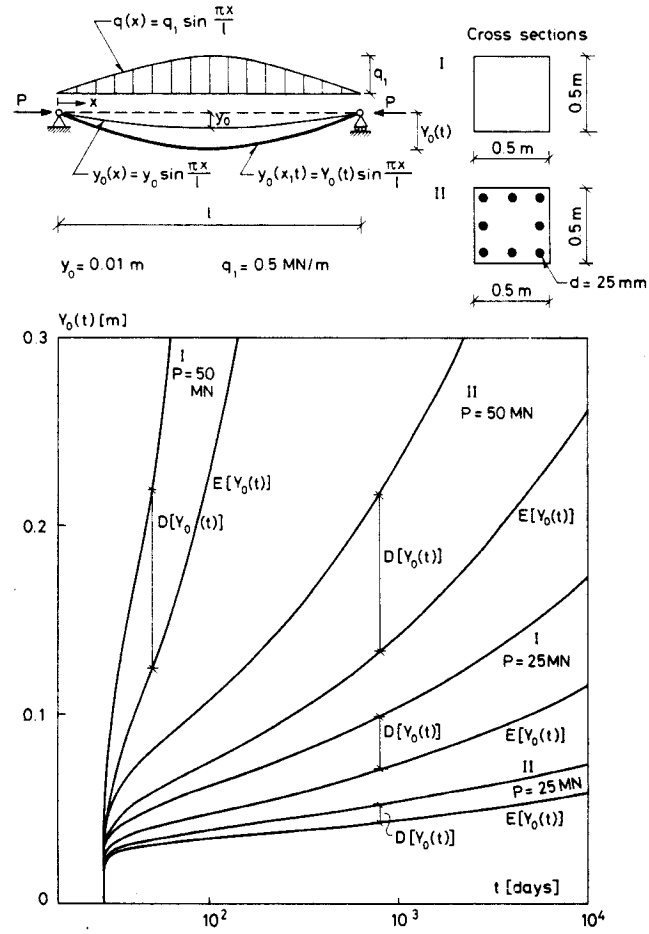

Fig. 9 — Creep buckling

cross-sectional constants are $A_c = 1650$ cm² (255.1 in.²), $A_s = 94.9$ cm² (14.71 in.²), $I_c = 14210$ cm⁴ (341.4 in.⁴), $I_s = 33300$ cm⁴ (800 in.⁴), $e = 0.279$ m (10.98 in.), and the modulus of steel is $E_s = 210{,}000$ MN/m² (30.46×10^6 psi). Shrinkage and creep parameters are given in Table 6(f). Fig. 8 shows the results for the steel bending moment. Deflections are proportional to the steel bending moment.

Creep buckling deformations

Fig. 9 shows the deformations at midspan of a slender concrete beam-column with square cross section. The column has a small initial sinusoidal curvature of amplitude y_o. The beam-column is subjected to an axial load P and a lateral sinusoidal load of amplitude q_1, both of which can vary in time. Two cross sections, one with and one without reinforcement, are considered. Ordinary beam-column theory is used and reinforcement is assumed linearly elastic. If the concrete is modeled as linearly elastic and the loads are constant in time, the differential equation for the deflection $y(x)$ is then[4]

$$(E_cI_c + E_sI_s)\,[y''(x) - y_o''(x)] = -Py(x) - \frac{l^2}{\pi^2}\,q(x) \tag{53}$$

The corresponding matrix equation for linear viscoelastic concrete and for time-varying loads is

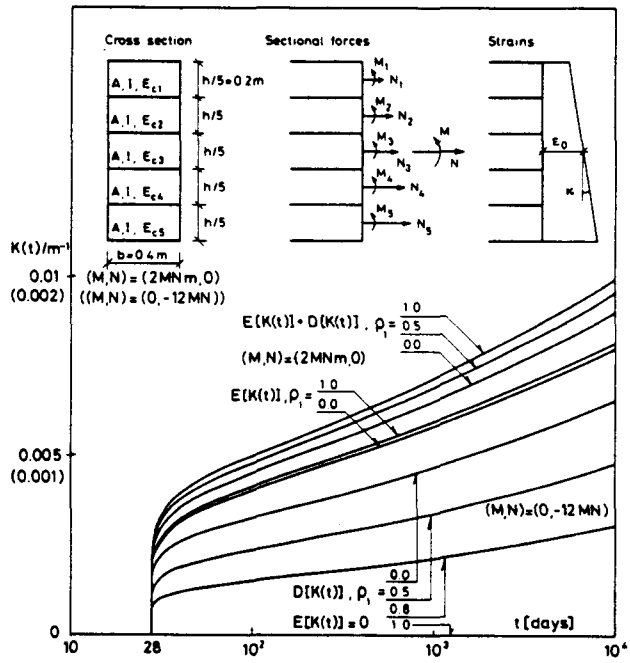

Fig. 10 — Curvature of 5-layer beam

$$(E_cI_c + E_sI_sI)\,[y''(x) - y_o''(x)e] = -Py(x) - \frac{l^2}{\pi^2}q(x) \tag{54}$$

where P is a diagonal matrix with elements $P(t_i)$ and e is a column matrix with all elements equal to 1. The solution to Eq. (54) is

$$y(x) = \left(\frac{\pi^2}{l^2}E_cI_c + E_sI_sI - P\right)^{-1} \left[\frac{l^2}{\pi^2}q(x) + \frac{\pi^2}{l^2}y_o(x)(E_cI_c + E_sI_sI)e\right] \tag{55}$$

Parameter values are given in Table 6(g), and results for the midpoint deflection are shown in Fig. 9. A considerable reduction of the standard deviation is noted when reinforcement is added to the cross section.

Beam split in five layers

The effect on the uncertainty of variations of the creep function across a sectional area is illustrated in this example. As shown in Fig. 10, a concrete beam is considered to consist of five layers of thickness $h/5$. The creep function can vary between layers, but the concrete within each layer is assumed homogeneous. The statistical properties of concrete in all layers are considered to be identical. Cross-sectional forces consist of a bending moment M and an axial force N which can both vary in time. The equilibrium conditions are, in matrix notation

$$\left.\begin{aligned} N &= N_1 + N_2 + N_3 + N_4 + N_5, \\ M &= M_1 + M_2 + M_3 + M_4 + M_5 \\ &\quad + (N_5 - N_1)\frac{2h}{5} + (N_4 - N_2)\frac{h}{5} \end{aligned}\right\} \tag{56}$$

The concrete strain distribution is assumed to be planar, and the stress-strain relations are

$$\epsilon(y) = E_{ci}^{-1}\sigma_i(y) \quad (i = 1, 2, \ldots, 5) \tag{57}$$

where σ_i is the stress in the i-th layer. The concrete stresses must be linearly distributed

$$\sigma_i(y) = \frac{N_i}{A} + \frac{M_i}{I_i}\left(y - \frac{i-3}{5}h\right) \quad (i = 1, 2, \ldots, 5) \tag{58}$$

From these equations the curvature $\kappa = E_{ci}M_i/I$ is calculated

$$\kappa = \frac{1}{I}[(E_{c1} + 11E_{c2} + E_{c3} + 37E_{c4} + 97E_{c5}) - 12(2E_{c5} + E_{c4} - E_{c2} - 2E_{c1})(E_{c1} + E_{c2} + E_{c3} + E_{c4} + E_{c5})^{-1}(E_{c2} + 2E_{c3} + 3E_{c4} + 4E_{c5})]^{-1} \left\{M - \frac{h}{5}(2E_{c5} + E_{c4} - E_{c2} - 2E_{c1})(E_{c1} + E_{c2} + E_{c3} + E_{c4} + E_{c5})^{-1}N\right\} \tag{59}$$

The parameter values used are given in Table 6(h). For simplicity, all variables except the model uncertainty factors Ψ_i are taken as deterministic and identical for all five layers. The mean values as well as the coefficients of variation for the five Ψ_i factors are taken to be identical. The Ψ_i factors are further taken equicorrelated with correlation coefficient ρ_1.

In Fig. 10 results for the curvature are shown for various combinations of the cross-sectional forces and for various values of ρ_1. The value of ρ_1 does not affect the mean curvature but can have a large effect on the variance of the curvature. The effect is, however, opposite for the cases of pure bending and pure axial load.

CONCLUSIONS

1. The random variability of creep and shrinkage effects in concrete structures is often very large and should be accounted for in design. Determining the variance functions for the structural variables of interest is probably sufficient for design.

2. Any chosen deterministic model for predicting creep and shrinkage can be randomized by considering the entering parameters as random variables and by also inserting uncertainty factors that characterize inadequacy of the chosen model.

3. Uncertainty in the internal forces and deformations of the structure can be efficiently obtained by point estimates of probability moments based on a number of usual deterministic structural analyses. This can be conveniently carried out in a matrix form.

4. Numerical examples show that certain internal forces or deformations which almost vanish in a deterministic analysis can have a very large uncertainty, which

should be accounted for in design. In some other cases, a large uncertainty in the entering parameters may cause only a small uncertainty in the internal force or deformation. The coefficient of variation can substantially vary with time.

ACKNOWLEDGMENT

This study was sponsored under the U.S. National Science Foundation Grant No. CEE8009050 to Northwestern University, which also supported H. Madsen's stay at the university in 1981. Mary Hill is thanked for her superb secretarial assistance.

CONVERSION FACTORS

1 m = 100 cm = 39.37 in.
1 MPa = 145.0 psi
1 MNm = 10^6 Nm = 8.851 lbf × in.

NOTATION

a_1, c	=	coefficients defined in Table 1
Cov	=	covariance
D	=	effective thickness
E	=	expectation
E_c	=	elastic modulus of concrete
E_c	=	square matrix in Eq. (17)
f'_c	=	standard 28 day cylinder strength
g/c, h, h_o, k_s	=	coefficients defined in Table 1
I	=	centroidal moment of inertia
$J(t,t')$	=	compliance function of concrete [Eq. (2) and (13)]
L	=	square matrix in Eq. (16)
s	=	standard derivation
s/c	=	sand-cement ratio (by weight)
t	=	time = age of concrete
t'	=	age at loading
t_o	=	age when drying begins
t_i	=	discrete times [Eq. (14)]
T	=	temperature
V	=	coefficient of variation
w/c	=	water-cement ratio (by weight)
ϵ, ϵ_i	=	strain, and strain at t_i
ϵ_{sh}, ϵ^0	=	shrinkage strain and inelastic strain
θ, θ_i	=	random variables
ρ_{ij}	=	corelation coefficients
σ, σ_i	=	stress, and stress at t_i
Ψ, Ψ_i	=	model uncertainty coefficients [Eq. (4) and (8)]

REFERENCES

1. Ditlevsen, O., "Stochastic Visco-Elastic Strain Modeled as a Second Moment White Noise Process," *International Journal of Solids and Structures,* V. 18, No. 1, 1982, pp. 23-25.

2. Tsubaki, T., and Bažant, Z. P., "Random Shrinkage Stresses in Aging Viscoelastic Vessel," *Proceedings,* ASCE, V. 108, EM3, June 1982, pp. 527-545.

3. Çinlar, E.; Bažant, Z. P.; and Osman, E., "Stochastic Process for Extrapolating Concrete Creep," *Proceedings,* ASCE, V. 103, EM6, Dec. 1977, pp. 1069-1088.

4. Bažant, Z. P., and Najjar, J., "Comparison of Approximate Linear Methods for Concrete Creep," *Proceedings, ASCE, V. 99,* ST9, Sept. 1973, pp. 1851-1874.

5. Bažant, Z. P., and Panula, L., "Practical Prediction of Time-Dependent Deformations of Concrete," *Materials and Structures, Research and Testing* (RILEM, Paris), V. 11, No. 65, Sept.-Oct. 1978, pp. 307-328; V. 11, No. 66, Nov.-Dec. 1978, pp. 415-434; and V. 12, No. 69, May-June 1979, pp. 169-183.

6. Bažant, Zdeněk P., and Panula, Liisa, "Creep and Shrinkage Characterization for Analyzing Prestressed Concrete Structures," *Journal,* Prestressed Concrete Institute, V. 25, No. 3, May-June 1980, pp. 86-122.

7. Bažant, Z. P., "Input of Creep and Shrinkage Characteristics for a Structural Analysis Program," *Materials and Structures, Research and Testing* (RILEM, Paris), V. 15, No. 88, July-Aug. 1982, pp. 283-290.

8. Bažant, Z. P., "Mathematical Models for Creep and Shrinkage of Concrete," *Creep and Shrinkage of Concrete Structures,* Z. P. Bažant and F. H. Wittmann, Editors, John Wiley and Sons, London, 1982, pp. 163-256.

9. Bolomey, J., "Bestimmung der Druckfestigkeit von Mörtel und Beton," *Schweizerische Bauzeitung* (Zürich), 1926. Also, "Détermination de lâ résistance probable d'un béton," *Technique des Travaux* (Paris-Brussels), 1929.

10. Ditlevsen, O., *Uncertainty Modeling,* McGraw-Hill Book Company, New York, 1981, 304 pp.

11. Alou, F., and Wittmann, F. H., "Etude expérimentale de la variabilité de retrait du béton," *Preprint,* Symposium on Fundamental Research on Creep and Shrinkage of Concrete (Lausanne, Sept. 1980), Swiss Federal Institute of Technology, Lausanne, 1980, pp. 61-78.

12. Mullick, A. K., "Effect of Stress-History on the Microstructure and Creep Properties of Maturing Concrete," thesis, Department of Civil Engineering, University of Calgary, 1972.

13. Reinhardt, H. W.; Pat, M. G. M.; and Wittmann, F. H., "Variability of Creep and Shrinkage of Concrete," *Preprint,* Symposium on Fundamental Research on Creep and Shrinkage of Concrete (Lausanne, Sept. 1980), M. Nijhoff, The Hague, 1982, pp. 75-94.

14. Rosenblueth, E., "Point Estimates for Probability Moments," *Proceedings,* National Academy of Sciences, Mathematics, V. 72, No. 10, Oct. 1975, pp. 3812-3814.

15. Bažant, Z. P., "Numerical Determination of Long-Range Stress History from Strain History in Concrete," *Materials and Structures, Research and Testing* (RILEM, Paris), V. 5, No. 27, May-June 1972, pp. 135-141.

16. "Time Dependent Effects," *Finite Element Analysis of Reinforced Concrete,* American Society of Civil Engineers, New York, 1982, pp. 309-400.

17. Madsen, K., "Matrix Formulation for Practical Solution of Concrete Creep Problems," *DIALOG* 1-79, Danish Engineering Academy, Lyngby, 1979.

18. Madsen, H. O., and Ditlevsen, O., "On the Uncertainty of Concrete Creep," *DIALOG* 1-80, Danish Engineering Academy, Lyngby, 1980.